Study of Electrostatic Ion-Cyclotron Waves Around the Plasmapause including Effect of H$^+$, He$^+$ and O$^+$ Ions

Vibhooti khaira[#1] and G. Ahirwar*[2]

School of studies in physics,Vikram university,
Ujjain (M.P.) 456010, India

Abstract

In this paper, we have investigated of electrostatic ion cyclotron waves in multi-ions plasma (H$^+$, He$^+$ and O$^+$) using particle aspect analysis. The kappa distribution function, dispersion relation, growth rate have been derived for EIC waves in multi-ions plasma. The wave is assumed to propagate obliquely to the static magnetic field. It is observed that the effect of kappa distribution function in multi-ions (H$^+$, He$^+$ and O$^+$) of EIC waves is to enrich the growth rate. The advantages of present approach and study are to its suitability for allocating and defining the effect of kappa distribution function on EIC waves. The study may explain the EIC waves observed in this region and play a major role of particle density variation in particular region.

Keywords: *ESIC wave, multicomponent, plasmapause region, kappa distribution, dispersion relation, growth rate, perpendicular and parallel resonant energy.*

I. INTRODUCTION

The exterior boundary of theplasmasphere is mentioned to as the plasma-pause region where the plasma density has a sharpincline. Carpenter et al. (1)reported the locationof the plasma-pause linked to the region of enhanced trapped energetic electrons. Xinlin et al. (2) have rehabilitated interesting topographies about the plasma-pause region. Moldwin et al. (3) using CRRES satellite observations reported clear and sharp 'classic' isolated sharp density inclines and that plasma-pause observations with noteworthy structure or density cavities were more common. In the course of storm times, the pitch angle scattering of the radiation belt electrons is more prominent near and just exterior the plasma-pause where electrostatic ion cyclotron (ESIC) waves are also perceived.

ESIC waves with multi-ion play an imperative role in the inclusivedynamics of space plasmas. They not only act as a valuablediagnostic of the significant physical processes, but they can also disturb the macroscopic plasma state by manipulating the transport properties. These waves favorably generatedin high-density region.

The observational schoolwork by Xinlin et al. (2), Bortniket al. (4), Fuselier et al. (5) and Spasojevic et al.(6) be responsible for the authensity to our theoretical modelwhich describe the ESIC wave with multi-ion structure in plasma-pauseregion. The existinginvestigation is grounded upon (Dawson's,1961) theory of Landau damping which was furtherprolonged by Terashima (1967), Misra and Tiwari (1979),Varma and Tiwari (1992, 1993), Dwivedi et al. (2001,2002), Shandilya et al. (2003, 2004), Mishra and Tiwari(2006), Ahirwar et al. (2006, 2007) to the analysis ofelectrostatic and electromagnetic instabilities. The entireplasma is deliberated to contain of resonant and nonresonantparticles. Non-resonant particles sustenance theoscillatory motion of the EMIC waves whereas, theresonant particles contribute in the energy interchange withthe wave. An ESIC wave starts at t=0, when the resonantparticles are not troubled. Using the particle trajectory inthe existence of ESIC wave in multi-ion plasma, the dispersion relation andgrowth rate are derived and deliberated for differentdistribution indices and the thermal anisotropy aroundthe plasma-pause. In the currentschoolwork, we concentrate ourattention to describe the ESIC wave generation and energyallocation in the plasma-pause region accordance to theobservations by Solar, Anomalous, and MagnetosphericParticle Explorer [SAMPEX] and Combined Radiationand Release Experiment Satellite [CRRES] satellite.The gains of existing approach and schoolwork is to its appropriateness for allocating and determining the effect of kappa distribution on ESIC in magnetosphere and governs the properties of the medium (plasma) in magnetosphere.The hypotheticalschoolwork of ion heating and acceleration upright to the magnetic field are collective features in the auroral region.

The foremostintention of this schoolwork is to examine the generation of ESIC waves in the magnetosphere and perceive the effect of kappa

distribution in magnetospheric plasma. The comprehensiveexplanation and formulae for the dispersion relation and growth rate is resolute in the next section.

II. BASIC ASSUMPTION

The trajectories of particles are then evaluated within the framework of linear theory.

$$K_{\Pi} E, k = (k_{\perp}, 0, k_{\Pi}), \quad E = (E_x, 0, E_z)$$

With

$$E_x(r,t) = E_1 \cos(k_{\perp}x + k_{\Pi}z - \omega t),$$

$$E_z(r,t) = kE_1 \cos(k_{\perp}x + k_{\Pi}z - \omega t)$$

and

$$k = (\frac{k_{\Pi}}{k_{\perp}}) < 1$$

where

$$\phi = k_{\perp}x + k_{\Pi}z - \omega t$$

The amplitude E_1 is slowly varying function of t i.e $\frac{1}{E_1}(\frac{dE_1}{dt}) \ll \omega$

Here, k_{Π} and $k_{\perp}$ are the components of the wave vector along and across the magnetic field, respectively and ω represent the wave frequency.

A. Velocities of the Particle

The trajectories of particles are evaluated within the framework of linear theory. The equation of motion of a particle is given by,

$$m(\frac{dv}{dt}) = q[E + (\frac{1}{c})v \times B_0] \quad (1)$$

If E is considered to be a small perturbation i.e. E=E$_0$+E$_1$, velocity v can be expressed in terms of unperturbed velocity V and perturbed velocity u.
Then the trajectories of the free gyration are obtained

as,
$$X(t) = \frac{V_{\perp}}{\Omega_{\alpha}}[\sin(\theta - \Omega_{\alpha}t) - \sin\theta] + Y_0.$$

$$Y(t) = \frac{V_{\perp}}{\Omega_{\alpha}}[\cos(\theta - \Omega_{\alpha}t) - \cos\theta] + Y_0. \quad (2)$$

$$Z(t) = V_{\Pi}t + Z_0.$$

The perturbed velocity u is determined by;

$$\frac{du_{\perp}}{dt} + i\Omega_{\alpha}u_{\perp} = \frac{qk_{\Pi}E_1}{k_{\perp}m}\sum_{-\infty}^{+\infty} J_1(\mu)\cos(A_{\lambda}t + \psi_{\lambda}^0) \quad (3)$$

$$\frac{du_{\Pi}}{dt} = \frac{qE_1}{m}\sum_{-\infty}^{+\infty} J_1(\mu)\cos(A_{\lambda}t + \psi_{\lambda}^0)$$

Where $u_{\perp} = u_x + iu_y$ represents the perturbed velocity in transverse direction and $u_{\parallel}$ represents the velocity in parallel direction. The resonance criteria are given by;

$$A_{\lambda}(V_{\Pi} = V_r) = k_{\Pi}V_{\Pi} - \omega + \lambda\Omega_{\alpha} = 0; \lambda = \pm 1, \pm 2, \pm 3, \dots \dots$$

Here, V_r is the resonance velocity of the particles.
The oscillatory solution of u (t) is given by;

$$u_x(\vec{r}.t) = -\frac{qE_1}{m}\sum_{-\infty}^{+\infty} J_n(\mu) \times \left[\frac{A_{\lambda}}{A_{\lambda} - \Omega_{\alpha}^2}\sin\chi_{nl} - \frac{\delta}{2A_{n+1}}\sin(\chi_{nl} - A_{n+1}t) - \frac{\delta}{2A_{n-1}}\sin(\chi_{nl} - A_{n-1}t) \right]$$

$$u_y(\vec{r}.t) = \frac{qE_1}{m}\sum_{-\infty}^{+\infty} J_n(\mu)\sum_{-\infty}^{+\infty} J_{\lambda}(\mu) \times \left[\frac{A_{\lambda}}{A_{\lambda}^2 - \Omega_{\alpha}^2}\cos\chi_{nl} - \frac{\delta}{2A_{n+1}}\cos(\chi_{nl} - A_{\lambda+1}t) \right.$$

$$\left. - \frac{\delta}{2A_{\lambda-1}}\sin(\chi_{nl} - A_{\lambda-1}t) \right]$$

$$u_z(\vec{r}.t) = \frac{qk_{\Pi}E_1}{k_{\perp}m}\sum_{-\infty}^{+\infty} J_n(\mu)\sum_{-\infty}^{+\infty} J_{\lambda}(\mu) \times \frac{1}{A_{\lambda}}\left[\sin\chi_{nl} - \delta\sin(\chi_{nl} - A_{n+1}t) \right]$$

(4)

Here
$$\chi_{nl} = k.r - \omega t + (n - \lambda)(\Omega_{\alpha}t - \theta)$$

$\delta = 0$ for non-resonant particles and $\delta = 1$ for resonant particles.

B. Distribution Function

To determine the dispersion relation and growth rate, we consider bi-Maxwellian plasma as,

$$f_0(y,V) = N_0 f_{\perp}(V_{\perp}) f_{\Pi}(V_{\Pi}) \quad (5)$$

We consider a general loss-cone distribution function for $f_{\perp}(V_{\perp})$ as

$$f_{\perp}(V_{\perp}) = \left[\frac{V_{\perp}^{2J}}{\pi V_{T\perp}^{2(J+1)}} \right] \exp\left(-\frac{V_{\perp}^2}{V_{T\perp}^2} \right) \quad (6)$$

And $f_{\parallel}(V_{\parallel})$ which is defined by the drifting Maxwellian as $f_{\Pi}(V_{\Pi}) = \left[\frac{V_{\Pi}^{2J}}{\sqrt{\pi} V_{\Pi\perp}^{2(J+1)}} \right] \exp\left(-\frac{V_{\Pi}^2}{V_{T\Pi}^2} \right) \quad (7)$

Here using the value of $V_{T\perp}^2 = (J+1)^{-1}\frac{2T_{\perp}}{m}$ and $V_{T\Pi}^2 = \frac{2T_{\Pi}}{m}$ for plasma and the bi-lorentzian, which reduces to the anisotropic bi-maxwellian distribution when the spectral index k tends to infinity is given by,

$$F = \frac{1}{\sqrt[3]{\pi}} \frac{\Gamma(\kappa + J + 1)}{\sqrt[3]{\kappa}\,\Gamma\,\kappa - 1/2\,V^2{}_{T\perp}V^2{}_{TII}}$$

$$[1 + \frac{V^2{}_{T\perp}}{KV^2{}_{T\perp}} + \frac{V^2{}_{TII}}{KV^2{}_{TII}}]^{-(\kappa+J+1)}$$

(8)

In equation (8) $V^2{}_{T\perp}$ and $V^2{}_{TII}$ are related to the mass m and the temperatures $T_\perp$ and T_{II} respectively parallel and perpendicular to the magnetic field by,

$$V^2{}_{T\perp} = (J+1)^{-1}[\frac{\kappa - 3/2}{\kappa}\frac{2KT_\perp}{m}]$$

(9)

$$V^2{}_{TII} = [\frac{\kappa - 3/2}{\kappa}\frac{2KT_{II}}{m}]$$

(10)

The quasi-neutrality condition yields to the equation:

$$n_e = n_{H^+} + n_{He^+} + n_{O^+}$$

Thus we evaluate the density perturbation associated with the particle velocity as:

$$\frac{dn_1}{dt} = -F_{H^+}(V)(\nabla.u)_{H^+} + (-F_{He^+}(V)(\nabla.u)_{He^+} +$$

$$(-F_{O^+}(V)(\nabla.u)_{O^+}$$

(11)

The integration w.r.to t from equation (8) we get the solution for perturbed density as

$$n_1(r,t) = -\frac{qE_1 F(V_\alpha)}{m_\alpha k^2{}_\perp}k_{II}^2\sum_{-\infty}^{+\infty}J_\lambda(\mu)J_n(\mu)\times$$

$$[\frac{k_\perp}{A^2{}_\lambda - \Omega^2{}_\alpha} + \frac{k_{II}^2 K_\perp}{k^2{}_\perp A^2{}_\lambda}]\sin\chi_{nl}$$

And

$$n_1(r,t) = \frac{qE_1 F(V_{H^+})}{m_{H^+}k^2{}_\perp}k_{II}^2 K_\perp\sum_{\lambda,n=-\infty}^{+\infty}J_\lambda(\mu)J_n(\mu)\frac{1}{A^2{}_{\lambda H^+}}$$

$$\{\sin(\chi_{n\lambda} - \sin(\chi_{n\lambda} - A_{\lambda H^+}t) - A_{\lambda H^+}t\cos(\chi_{n\lambda} - A_{\lambda H^+}t)\} +$$

$$\frac{qE_1 F(V_{He^+a})}{m_{He^+}k^2{}_\perp}k_{II}^2 K_\perp\sum_{\lambda,n=-\infty}^{+\infty}J_\lambda(\mu)J_n(\mu)\frac{1}{A^2{}_{\lambda He^+}}$$

$$\{\sin(\chi_{n\lambda} - \sin(\chi_{n\lambda} - A_{\lambda He^+}t) - A_{\lambda He^+}t\cos(\chi_{n\lambda} - A_{\lambda He^+}t)\} +$$

(12)

$$\frac{qE_1 F(V_{O^+})}{m_{O^+}k^2{}_\perp}k_{II}^2 K_\perp\sum_{\lambda,n=-\infty}^{+\infty}J_\lambda(\mu)J_n(\mu)\frac{1}{A^2{}_{\lambda O^+}}$$

$$\{\sin(\chi_{n\lambda} - \sin(\chi_{n\lambda} - A_{\lambda O^+}t) - A_{\lambda O^+}t\cos(\chi_{n\lambda} - A_{\lambda O^+}t)\}$$

III. DISPERSION RELATION

We consider the cold plasma dispersion relation for the ESIC wave as

$$n_{\alpha,e} = \mp\int dvF(v)\frac{eE_1 K_\perp}{m_{\alpha,e}}\sum_{n\lambda}\left\{\begin{array}{c}J_\lambda(\mu)J_n(\mu)\times\\ \dfrac{K_\perp}{A^2{}_\lambda - \Omega^2{}_\alpha} + \dfrac{k_{II}^2}{k^2{}_\perp A^2{}_\lambda}]\sin\chi_{nl}\end{array}\right\}$$

(13)

Where $n_{\alpha,e}$ is integrated density and

$$\mu = \frac{K_\perp V_I}{\Omega_{\alpha,e}}, A = K_{II}V_{II} - \omega + n\Omega_{i,e}, \chi_{n\lambda} = k.r - \omega t + (n-l)(\Omega_\alpha l - \theta)$$

Using the expression, then the dispersion relation EIC waves in multi-component plasma is given by

$$n_e = (\frac{1}{k_\perp d^2{}_{IIe}})\frac{E_1}{4\pi e}\sin(kr - \omega t)$$

And

$$n_\alpha = -\frac{k_{II}^2\omega^2{}_{p\alpha}1}{(\omega - \lambda\Omega_\alpha)k_\perp}\left\langle 1 - \frac{k^2{}_\perp\rho^2{}_\alpha}{2}(\frac{2\kappa - 3}{\kappa})\right\rangle\frac{E_1}{4\pi e}\sin(kr - \omega t)$$

Where $\alpha = H^+, He^+, O^+$ and $\omega^2{}_{p\alpha} = \dfrac{4\pi N_\alpha e^2}{m_\alpha}$ is the

plasma frequency for multi-ions and N_α is the multi-ions plasma density.

Debye length ($d^2{}_{IIe}$) is given by

$$d^2{}_{IIe} = \frac{T_{IIe}}{m_e\omega^2{}_{pe}}$$

Using the Poisson's equation

$$\nabla.E = 4\pi e(n_\alpha - n_e)$$

(14)

The perturbed ion and electron density ni and ne the dispersion relation is obtain as

$$\omega = \Omega_\alpha + [\omega^2{}_{p\alpha}\left\langle 1 - \frac{k^2{}_\perp\rho^2{}_\alpha}{2}(\frac{2\kappa-3}{\kappa})\right\rangle(\frac{1}{\frac{k_\perp + k_{II}}{k^2{}_{II}k_\perp} + \frac{k^2{}_\perp}{k^2{}_{II}}(\frac{1}{k^2{}_\perp d^2{}_{IIe}})})]$$

(15)

IV. WAVE ENERGY AND GROWTH RATE

The wave energy W_w per unit wavelength is the sum of the pure field energy. The total energy per unit wavelength is given as

$$W_w = \frac{\lambda B^2}{8\pi} + W_e + W_{r\alpha}$$

Where $W_e = \frac{\lambda E^2}{8\pi} + \frac{\lambda E^2}{16\pi}(\frac{1}{k_\perp d^2{}_{IIe}})$

$$W_{r\alpha} = \sum_\alpha (W_{r\alpha\perp} + W_{r\alpha II})$$

and

$$W_{r\perp} = \int_0^\lambda dz\int_0^\infty V_{\perp\alpha}dV_{\perp\alpha}\int_0^{2\theta}d\theta\int_{v_r - \Delta r}^{v_r + \Delta r}dV_{II\alpha}\frac{m}{2}[(N + n_{1\alpha})(V_{\perp\alpha} + u_{\perp\alpha})^2 - NV_{\perp\alpha}^2]$$

(16)

$$W_{rII} = \int_0^\lambda dz \int_0^\infty V_{IIa} dV_{IIa} \int_0^{2\theta} d\theta \int_{v_r - \Delta r}^{v_r + \Delta r} dV_{\Pi a} \frac{m}{2}[(N + n_{1a})(V_{IIa} + u_{IIa})^2 - NV_{IIa}^2]$$

and Gurnett, 1978; Varma and Tiwari, 1991; Tiwari and Varma, 1993).

A. Perpendicular Resonant Energy

$$W_{r\perp a} = (\frac{\lambda E^2}{8\pi})(\frac{\omega_{pa}^2}{\Omega_a^2})(\frac{\omega}{k_{II}V_{tha}})\frac{\Omega_a t}{\sqrt{2\pi}}\exp\left\{-\frac{1}{2}(\frac{\omega}{k_{II}V_{tha}})^2(1-\frac{\lambda\Omega_a}{\omega})^2\right\}$$

$$\times \frac{1}{2}\left\langle 1 - \frac{k_\perp^2 \rho_a^2}{2}(\frac{2\kappa-3}{\kappa})\right\rangle \tag{17}$$

$$\left[1 - (\frac{R(\frac{\lambda\Omega_a}{\omega}-1)}{\frac{\lambda\Omega_a}{\omega}})\frac{T_{\perp a}}{T_{IIa}}\right]$$

$n_0 =500 cm^{-1}$; $B_0 = 600$; $\gamma = 6\times10^{-7} wb/m^2$; $\rho_i = 170 m$; and A$=\frac{T_{\perp a}}{T_{\|a}}$ for multi-ions, here α=H$^+$, He$^+$, O$^+$

Fig 1 shows that the variation of wave frequency (ω) sec^{-2} versus wave vector $k_\perp$ (cm^{-1}) for different values of kappa distribution k = 1, 2, 3, 4. Here we have seen that at minimum value of kappa we get maximum growth rate corresponding to wave length. As we increase the value of kappa we get minimum peak of growth rate.

B. Parallel Resonant Energy

$$W_{rIIa} = (\frac{\lambda E^2}{8\pi})(\frac{\omega_{pa}^2}{\Omega_a^2})(\frac{\omega}{k_{II}V_{tha}})\frac{\Omega_a t}{\sqrt{2\pi}}\exp$$

$$\left\{-\frac{1}{2}(\frac{\omega}{k_{II}V_{tha}})^2(1-\frac{\lambda\Omega_a}{\omega})^2\right\} \times \frac{1}{2}\left\langle 1 - \frac{k_\perp^2 \rho_a^2}{2}(\frac{2\kappa-3}{\kappa})\right\rangle$$

$$\left[(\frac{(\frac{\lambda\Omega_a}{\omega}-1)}{\frac{\lambda\Omega_a}{\omega}})\frac{T_{\perp a}}{T_{IIa}}\right]$$

Fig 2 and 3 show that the variation of growth rate γ versus wave vector $k_\perp$ (cm^{-1}) for different values of temperature anisotropy of hydrogen ions ($A_{H+} = 50, 60, 70, 80$) for kappa distribution function k=1 and 2. Here we found the effect of kappa, we get maximum peak of growth rate at maximum anisotropy of hydrogen ions for k=1. It implies that decreasing the value of temperature anisotropy of hydrogen ions, we get minimum growth rate.

$$\tag{18}$$

Where

$$R = \frac{1 - \frac{1}{2}\frac{k_\perp^2 \rho_a^2}{2}(\frac{2\kappa-3}{\kappa})}{1 - \frac{k_\perp^2 \rho_a^2}{2}(\frac{2\kappa-3}{\kappa})} \text{ and} \alpha = H^+, He^+, O^+$$

Fig 4 and 5 show that the variation of growth rate γ versus wave vector $k_\perp$ (cm^{-1}) for different values of temperature anisotropy of helium ions ($A_{He+} = 50, 60, 70, 80$) for kappa distribution function k=1 and 2. Here we have seen almost same effect of kappa distribution and temperature anisotropy of hydrogen ions. It implies thatmaximum value of temperature anisotropy of helium ions we get maximum growth rate of helium ions.

C. Growth Rate
Using the law of conservation of energy the growth rate is obtained as

$$\frac{\gamma}{\omega} = \sqrt{\frac{\pi}{2}}(\frac{\omega}{k_{II}V_{tha}})(1-\frac{\lambda\Omega_a}{\omega})^2\exp\left\{-\frac{1}{2}(\frac{\omega}{k_{II}V_{tha}})^2(1-\frac{\lambda\Omega_a}{\omega})^2\right\}\times$$

$$\left[R(\frac{\frac{\lambda\Omega_a}{\omega}-1}{\frac{\lambda\Omega_a}{\omega}})\frac{T_{\perp a}}{T_{IIa}}-1\right] \tag{19}$$

V. RESULT AND DISCUSSIONS

We have calculated the growth rate, resonance energies and dispersion relation using the following plasma-pause parameters. (Hasegawa, 1971; Kintner
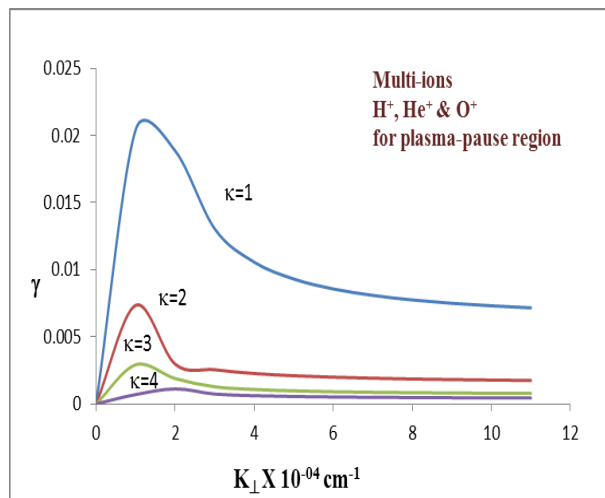
Fig 1 shows the variation of wave frequency (ω) sec^{-2} versus wave vector $k_\perp$ (cm^{-1}) for different values of kappa distribution k = 1, 2, 3, 4.
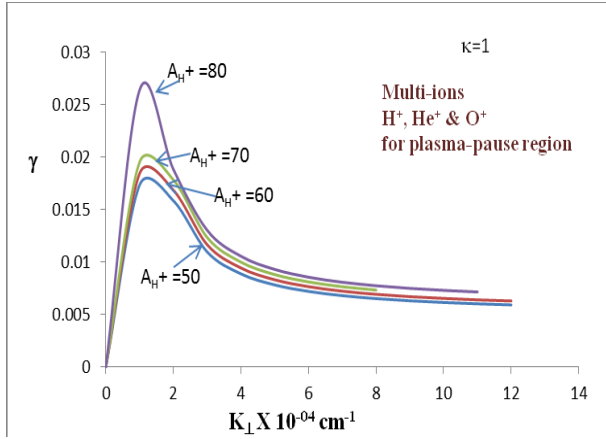
Fig 2 shows the variation of growth rate γ versus wave vector $k_\perp$ (cm^{-1}) for different values of temperature anisotropy of hydrogen ions ($A_{H+} = 50, 60, 70, 80$) for kappa distribution function k=1.
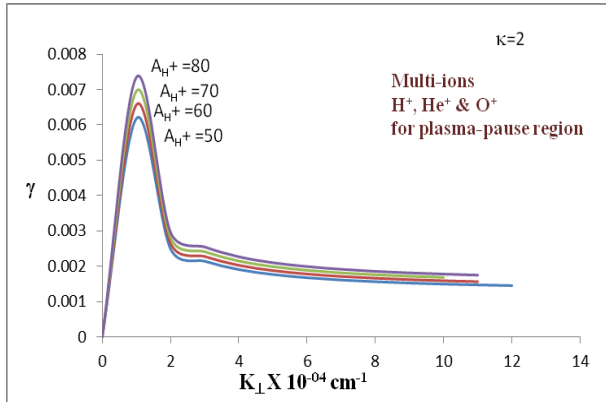
Fig 3 shows the variation of growth rate γ versus wave vector $k_\perp$ (cm^{-1}) for different values of temperature anisotropy of hydrogen ions ($A_{H+} = 50, 60, 70, 80$) for kappa distribution function k=2.
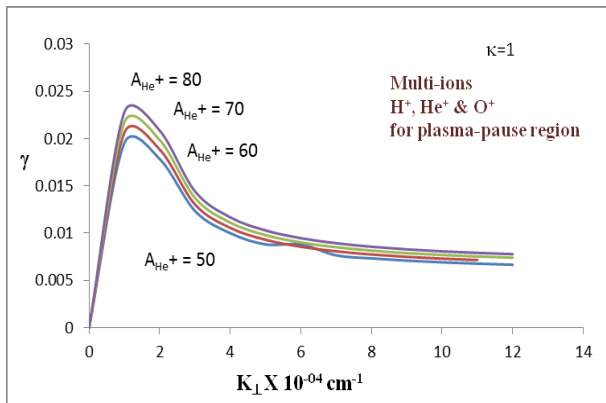
Fig 4 shows the variation of growth rate γ versus wave vector $k_\perp$ (cm^{-1}) for different values of temperature

anisotropy of helium ions ($A_{He+} = 50, 60, 70, 80$) for kappa distribution function k=1.
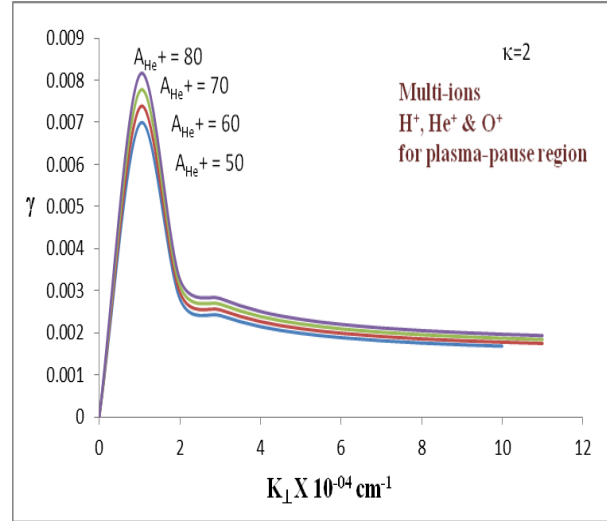
Fig 5 shows the variation of growth rate γ versus wave vector $k_\perp$ (cm^{-1}) for different values of temperature anisotropy of helium ions ($A_{He+} = 50, 60, 70, 80$) for kappa distribution function k=2.
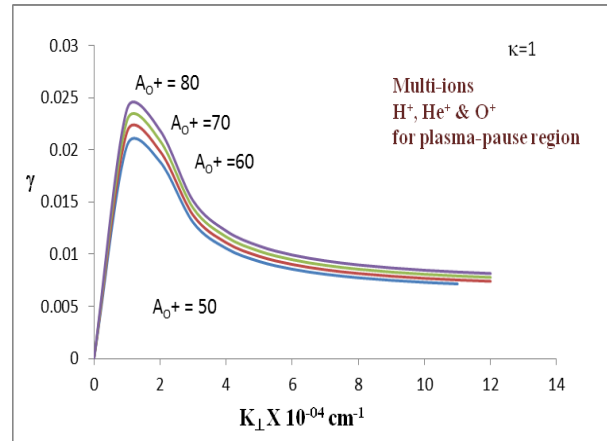
Fig 6 shows the variation of growth rate γ versus wave vector $k_\perp$ (cm^{-1}) for different values of temperature anisotropy of oxygen ions ($A_{o+} = 50, 60, 70, 80$) for kappa distribution function k=1.

Fig 6 and 7 show that the variation of growth rate γ versus wave vector $k_\perp$ (cm^{-1}) for different values of temperature anisotropy of oxygen ions ($A_{o+} = 50, 60, 70, 80$) for kappa distribution function k=1 and 2. Here again see same effect of temperature anisotropy of oxygen ions. At maximum value of temperature anisotropy, we get maximum growth rate at k = 1.Initially growth rate increases than decreases with respect to wave vector.
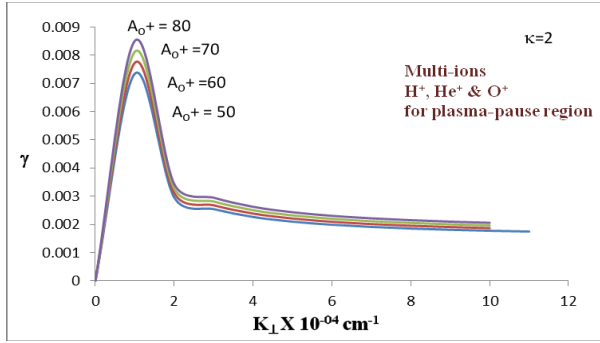
Fig 7 shows the variation of growth rate γ versus wave vector $k_\perp$ (cm^{-1}) for different values of temperature anisotropy of oxygen ions ($A_{o+} = 50, 60, 70, 80$) for kappa distribution function k=2.
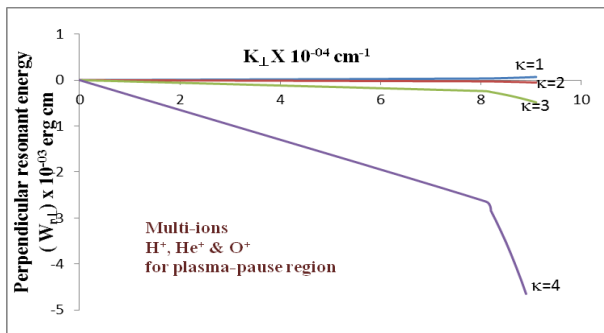
Fig 8 shows Variation of perpendicular resonant energy $W_{r\perp}$(erg cm) versus perpendicular wave vector $K_\perp$ (cm^{-1}) for different values of kappa distribution function (k=1, 2, 3 and 4).

Fig 8 shows that variation of perpendicular resonant energy $W_{r\perp}$(erg cm) versus perpendicular wave vector $K_\perp$ (cm^{-1}) for different values of kappa distribution function (k=1, 2, 3 and 4). The minimum value of kappa (k=1), we get maximum perpendicular resonant energy. But increasing value of kappa, we get decreasing perpendicular resonant energy.
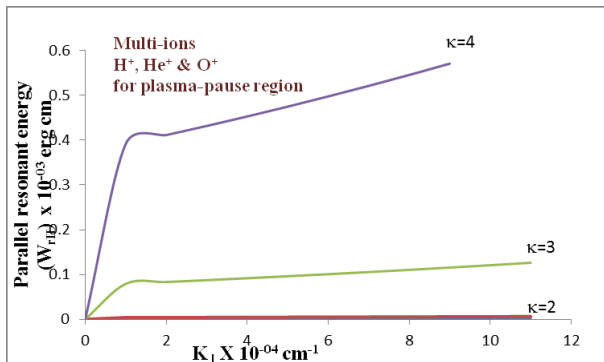
Fig 9 shows Variation of parallel resonant energy $W_{r\parallel}$(erg cm) with perpendicular wave vector $K_\perp$ (cm^{-1})

for different values of kappa distribution function (k=1, 2, 3 and 4).

Fig 9 depicts that the variation of parallel resonant energy $W_{r\parallel}$(erg cm) with perpendicular wave vector $K_\perp$ (cm^{-1}) for different values of kappa distribution function (k=1, 2, 3 and 4). Here we found that initially there is no resonant energy by the effect of kappa values (k=1 and 2) but as we increase the value of kappa (k= 3 and 4) first we get linear energy then approximately constant parallel resonant energy with respect to wave vector.

This one is perceived that the growth rate of ion-cyclotron wave arises by take-out energy from particles affecting perpendicular to the magnetic field. Therefore, the locked and conversing dipolar magnetic field lines at plasma-pause may allow the kappa distribution function and the ESIC waves are motivated by take-out perpendicular energy of the ions. The rise in parallel component of energy of ions with distribution indices k is observed in. The energy allocation from perpendicular to the parallel direction is observed along with the generation of ESIC waves at higher kappa distribution indices.

VI. CONCLUSION

In this paper, we studied **electrostatic ion-cyclotron waves around the plasmapause including effect of H$^+$, He$^+$ and O$^+$ ions.** We have accompanied an inclusive mathematical investigation.

The ending comments of this schoolwork are as follows;

1- It is found that effect of increasing the values of kappa distribution is to enhance the growth rate of ESIC waves in multi-ions, may be due a fluctuating of the resonance condition.

2- It is observed that for k=1, growth rate of all multi-ion (H$^+$, He$^+$ and O$^+$) of temperature anisotropy has approximately same behavior and for k=2, growth rate of all multi-ion of temperature anisotropy has near about same nature.

3- In plasma-pause region, parallel resonant energy is maximum for different value of kappa distribution function with respect to wave vector and perpendicular resonant energy is minimum for all values of kappa.

4- In point of view of the remarks of ESIC wave around the plasma-pause our hypothetical research specified that the ESIC wave emissions and the associated phenomena can be appropriately pronounced considering the kappa distribution function in the anisotropic plasma which may be the cause of ring current destabilization and pitch angle scattering.

5- The behavior studied for the ESIC waves may be of importance in the electrostatic emission in the plasmapause region. The result of the study is also applicable to the plasma devices that have the kappa distribution.

REFERENCES

[1] Carpenter, D.L., Park, C.G., Arens, J.F., Williams, D.J., 1971. Position of the plasmapause during a stormtime increase in trapped energetic (Eo280 kev) electrons. J. Geophys. Res. 76, 4669.

[2] Xinlin, Li., Baker, D.N., O'Brien, T.P., Xie, L., Zong, Q.G., 2006. Correlation between the inner edge of outer radiation belt electrons and the innermost plasmapause location. Geophys. Res. Lett. 33, L14107.

[3] Moldwin, M.B., Downward, L., Rassoul, H.K., Amin, R., Anderson, R.R., 2002. A new model of the location of the plasmapause: CRRES results. J. Geophys. Res. 107 (A11), 1339.

[4] Bortnik, J., Thorne, R.M., O'Brien, T.P., Green, J.C., Strongeway, R.J., Shprits, Y.Y., Baker, D.N., 2006. Observation

[12] distribution function—particle aspect analysis. Ind. J. Pure Appl. Phys. 31, 616.

[13] Shandilya, R.P., Varma, P., Tiwari, M.S., 2003. Study of kinetic Alfven wave in the magnetized dusty plasma. Ind. J. Phys. 77B (5), 553.

[14] Shandilya, R.P., Varma, P., Tiwari, M.S., 2004. Kinetic Alfven wave in inhomogeneous anisotropic dusty magnetosphere with inhomogeneous electric field—particle aspect analysis. Ind. J. Radio Space Phys. 30, 24.

[15] Mishra, R., Tiwari, M.S., 2006. Effect of parallel electric field on electrostatic ion cyclotron instability in anisotropic plasma in the presence of ion beam and general distribution function. Planet. Space Sci. 54, 188.

[16] Dwivedi, A.K., Varma, P., Tiwari, M.S., 2001. Kinetic Alfven wave in the presence of parallel electric field in an inhomogeneous magnetosphere. Ind. J. Phys. 75B (6), 555.

[17] Dwivedi, A.K., Varma, P., Tiwari, M.S., 2002. Ion and electron beam effects on kinetic Alfven wave in an inhomogeneous magnetosphere. Planet. Space Sci. 50, 93.

[18] Ahirwar, G., Varma, P., Tiwari, M.S., 2006. Study of electromagnetic ioncyclotron instability in the presence of a

of two distinct, rapid loss mechanisms during the 20 November 2003 radiation belt dropout event. J. Geophys. Res. 111, A12216.

[5] Fuselier, S.A., Gary, S.P., Thomsen, M.F., Claflin, E.S., Hubert, B., Sandel, B.R., Immel, T., 2004. Generation of transient dayside subauroral proton precipitation. J. Geophys. Res. 109, A12227.

[6] Spasojevic, M., Frey, H.U., Thomsen, M.F., Fuselier, S.A., Gary, S.P., Sandel, B.R., Inan, U.S., 2004. The link between a detached subauroral proton arc and a plasmaspheric plume. Geophys. Res. Lett. 31, L04803.

[7] Terashima, Y., 1967. Particle aspect analysis of drift instability. Prog. Theor. Phys. 37, 775.

[8] Mishra, K.D., Tiwari, M.S., 1979. Particle aspect analysis of electromagnetic ion-cyclotron instability. Can. J. Phys. 57, 1124.

[9] Varma, P., Tiwari, M.S., 1991. Drift waves in the presence of inhomogeneous electric field with different distribution functions— particle aspect analysis. Phys. Scripta 44, 269.

[10] Varma, P., Tiwari, M.S., 1992. Ion and electron beam effects on drift wave instability with different distribution function— particle aspect analysis. Phys. Scripta 45, 275.

[11] Varma, P., Tiwari, M.S., 1993. Drift wave in the presence of an AC electric field with different parallel electric field with general loss-cone distribution function—particle aspect analysis. Ann. Geophys. 24, 1919.

[19] Ahirwar, G., Varma, P., Tiwari, M.S., 2007. Beam effect on electromagnetic ion-cyclotron waves with general loss-cone distribution function in an anisotropic plasma—particle aspect analysis. Ann. Geophys. 25, 557.

[20] Hasegawa, A., 1971. Drift wave instability at the plasmapause. J. Geophys. Res. 76, 5361.

[21] Kennel, C.F., Engelmann, F., 1966. Velocity space diffusion from work plasma turbulence in a magnetic field. Phys. Fluids 9, 2377.

[22] Kintner, P.M., Gurnett, D.A., 1978. Evidence of drift waves at the plasmapause. J.Geophys. Res. 83, 39.